fixation," *J. Neurochem.*, vol. 26, p. 423, 1976.
[5] R. H. Lenox, H. L. Wray, G. J. Balcom, T. D. Hawkins, and J. L. Meyerhoff, "Regional brain levels of cyclic nucleotides, gamma aminobutyric acid (GABA) and glutamate during chronic barbiturate ingestion and withdrawal," *Soc. for Neuroscience Abstr.*, p. 448, 1975.
[6] A. Guidotti, D. L. Cheney, M. Trabucchi, M. Duteuchi, and C. Wang, "Focussed microwave radiation: A technique to minimize postmortem changes of cyclic nucleotides, DOPA and choline and to preserve brain morphology," *Neuropharm.*, vol. 13, p. 1115, 1974.
[7] F. F. Weight, G. Petzold, and P. Greengard, "Guanosine 3′,5′-monophosphate in sympathetic ganglia: Increase associated with synaptic transmission," *Science*, vol. 186, p. 942, 1974.
[8] G. R. Siggins, E. F. Battenberg, B. J. Hoffer, F. E. Bloom, and A. L. Steiner, "Noradrenergic stimulation of cyclic adenosine monophosphate in rat purkinje neurons: An immunocytochemical study," *Science*, vol. 179, p. 585, 1973.
[9] C. C. Mao, A. Guidotti, and E. Costa, "Interactions between γ-aminobutyric acid and guanosine cyclic 3′,5′-monophosphate in rat cerebellum," *Molec. Pharm.*, vol. 10, p. 735, 1974.
[10] R. H. Lenox, O. P. Gandhi, J. L. Meyerhoff, and H. M. Grove, "A microwave applicator for *in vivo* rapid inactivation of enzymes in the central nervous system," *IEEE Trans. Microwave Theory Tech.*, vol. 24, p. 58, 1976.
[11] R. H. Lenox, J. L. Meyerhoff, O. P. Gandhi, and H. L. Wray, "Microwave inactivation; Pitfalls in determination of regional levels of cyclic AMP in rat brain," *J. Cyclic Nucleotide Res.*, vol. 3, p. 367, 1977.
[12] K. Keim and E. B. Sigg, "Plasma corticosterone and brain catecholamines in stress: Effect of psychotropic drugs," *Pharmacol. Biochem. Behav.*, vol. 4, p. 289, 1976.
[13] R. H. Lenox, J. L. Meyerhoff, G. J. Kant, G. R. Sessions, L. L. Pennington, and E. H. Mougey, "Differing neurochemical and hormonal responses to specific stressors," in *Soc. for Neurosciences 7th Annu. Meet.*, Abstract, 1121, 1977.
[14] M. M. Nachlas, "Cytochemical demonstration of succinic dehydrogenase by the use of a new *p*-nitrophenyl substituted ditetrazole," *J. Histochem. Cytochem.*, vol. 5, p. 420, 1957.
[15] S. G. Butcher and L. L. Butcher, "Acetylcholine and choline levels in the rat corpus striatum after microwave irradiation," *Proc. West Pharmacol. Soc.*, vol. 17, p. 37, 1974.
[16] P. V. Brown, R. H. Lenox, and J. L. Meyerhoff, "Microwave enzyme inactivation system: Electronic control to reduce dose variability," *IEEE Trans. Biomed. Eng.*, vol. BME-25, pp. 205–208, Mar. 1978.

# The Electric-Field Probe Near a Material Interface with Application to the Probing of Fields in Biological Bodies

GLENN S. SMITH, MEMBER, IEEE

*Abstract*—**A theoretical model is formulated to determine the effect of an interface between different media on the response of an electric-field probe. The model used provides a "worst case" estimate of the interaction between the probe and the interface. The effect of the interface on the response of the probe is examined as a function of the size of the probe, the insulation on the probe, the load admittance at the terminals of the probe, the dissipation in the surrounding medium, and the spacing between the probe and the interface. The use of electrically small bare and insulated probes to measure the field in the interior of biological bodies is discussed as an example. Measured results are shown to be in general agreement with the theory.**

## I. Introduction

IN MANY APPLICATIONS an electric dipole is used as a probe to measure the component of an incident electric field parallel to its axis. When the dipole is located in an inhomogeneous body, such as a biological specimen, the response of the probe can change with its position as a result of the variation of the electrical constitutive parameters within the body. The constitutive parameters may be slowly varying continuous functions of the position or may change abruptly at a material boundary, such as at a muscle–fat interface or the boundary between tissue and air. Specifically, the response from the probe, i.e., the voltage $V$, is proportional to the component of the incident electric field parallel to its axis ($\hat{z}$)

$$V = K_e \boldsymbol{E}(\boldsymbol{r}) \cdot \hat{z} = K_e E_z(\boldsymbol{r}) \tag{1}$$

and the proportionality factor $K_e$ is a function of the constitutive parameters of the medium surrounding the probe ($\sigma_e, \epsilon_e, \mu \approx \mu_0$) including any abrupt changes in these parameters due to nearby boundaries. Note that the *incident field* $E_z(\boldsymbol{r})$ in (1) is the field at the point where the probe is located when the probe is absent; it is the field to be measured. The *total field* is the incident field plus the field that is scattered from the probe and scattered between the probe and the boundaries of the body.

Ideally, a probe is needed that has a proportionality

Manuscript received February 15, 1978; revised June 5, 1978.
The author is with the School of Electrical Engineering, Georgia Institute of Technology, Atlanta, GA 30332.

0018-9480/79/0300-0270$00.75 ©1979 IEEE

factor $K_e$ that is independent of the location of the probe within the inhomogeneous body. The voltage $V$ can then be interpreted as a measure of the electric field $E_z(r)$ without a specific knowledge of the constitutive parameters of the material in the immediate vicinity of the probe or the location of nearby boundaries. A probe with this response would be calibrated absolutely by measuring a known field in one standard medium, i.e., by determining $K_e$.

When the constitutive parameters of the body are a slowly varying continuous function of the position, the material in the immediate vicinity of an electrically small probe is approximately homogeneous. In this case, the variation of the probe's response with position, i.e., a change in $K_e$, is a result of a change in the constitutive parameters of the material surrounding the probe. In previous papers, the author showed that the response of both the bare and the concentrically insulated electrically short dipole probes under certain conditions could be made fairly independent of the constitutive parameters of the surrounding material [1], [2]. To obtain this independence for the electrically short bare dipole, the admittance of the load at its terminals must be much less than the admittance of the dipole, i.e., $|Y_L| \ll |Y|$. For the electrically short insulated dipole (the insulated probe is shown in Fig. 3), the response is fairly independent of the constitutive parameters of the medium if the ratio of the permittivity of the external medium to that for the insulation is large, $\epsilon_{er}/\epsilon_{eri} \gg 1$.

In this paper, the response of the dipole probe is examined when a boundary formed by an abrupt change in the constitutive parameters of the body (an interface) is nearby. For this case, the interaction between the probe and the interface is a result of the scattering of electromagnetic energy from the two elements. Note that, here, the mechanism altering the response of the probe is different from the one previously described. Rather than analyze each specific configuration for the probe and interface used in practice, a "worst case" analysis is used to determine the effect the interface has on the response $K_e$ of the probe.

The "worst case" analysis is used to provide a qualitative picture of how the various parameters, such as the length of probe, the insulation, the load admittance, and the distance from the interface, affect the response. The analysis can also be used to estimate the minimum separation required between the probe and the interface, if the difference (error) between the actual response (with the interface present) and that for a probe in an infinite medium (interface absent) is to be kept below a certain level.

In a recent exchange of comments between Bassen and Chen, the relative merits of changing the dipole length, adding insulation, and adjusting the load admittance were debated as means of reducing the interaction of an electric field probe with material boundaries in biological bodies [3]. The theoretical and experimental results presented in this paper provide quantitative information that answers some of the questions posed in their debate.

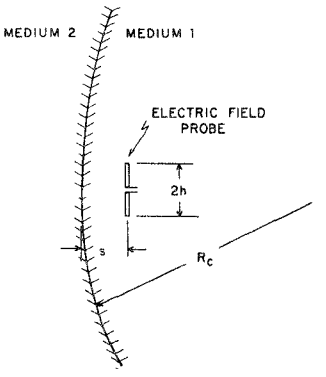


Fig. 1. Electric-field probe near an interface between media.

## II. Formulation of the Model Problem

The geometry for the electric field probe near an interface between two different media is shown in Fig. 1. If the probe is to be used to measure the distribution of the field in each of the media (1 and 2), its maximum dimension $2h$ must be small compared to the dimensions of the media. Specifically, when the radius of curvature describing the interface is $R_c$, then $2h \ll R_c$. If the distance between the probe and the interface is also small so that $s \ll R_c$, as it will be when the interaction between the probe and the interface is large, then the surface on the interface that is in the immediate vicinity of the probe is nearly planar. For an approximate analysis of the probe near an interface, the geometry shown in Fig. 1 can be replaced by a probe at a distance $s$ from a planar interface between the two media.

The maximum interaction between the probe and the interface will occur when the electrical properties of the media on the sides of the interface are very different and the probe is parallel to the interface. An extreme case will be considered here, namely, an interface between a dissipative medium (region 1) with the electrical constitutive parameters $\sigma_e, \epsilon_e, \mu_0$ and a perfect conductor (region 2); see Fig. 2(a). The effect this interface has on the performance of the probe is expected to be greater than would be produced if region 2 were a medium with a finite conductivity. The results obtained from the analysis of this interface are, therefore, considered to give a "worst case" estimate of the error introduced in the response of the probe by the presence of a nearby interface. For the calculation, the source of the electric field is assumed to be an incident electromagnetic plane wave with the electric field parallel to the axis of the probe and the plane of the interface,

$$E^i = \hat{z} E_0 e^{-jkx} \tag{2}$$

where $k = \beta - j\alpha$ is the wavenumber in the medium.

The method of images is now used to obtain an arrangement of sources and conductors which is equivalent to that in Fig. 2(a) for determining the electromagnetic field in the region $x \leqq 0$. This is shown in Fig. 2(b). The current in the image probe in Fig. 2(b) is in the direction opposite to that in the actual probe, i.e., $I' = -I$, and the image of the incident plane wave has the form

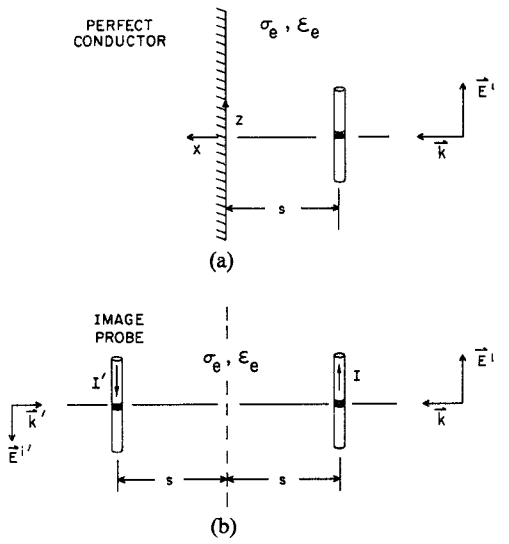


Fig. 2. (a) Probe parallel to a plane interface formed by a perfect conductor and a material. (b) Equivalent arrangement obtained using the method of images.

$$E^{i'} = -\hat{z}E_0 e^{jkx}. \tag{3}$$

The pair of nonstaggered parallel dipoles shown in Fig. 2(b) can be analyzed using the theory for coupled linear antennas in a dissipative medium [4]. The distribution for the total axial current $I(z)$ on the probe is given by the solution to the following integral equation:

$$\int_{-h}^{h} I(z')K_d'(z,z')\,dz' = \frac{j4\pi}{\zeta \cos kh} F_0(z). \tag{4}$$

The parameters that describe the bare linear antenna are shown in Fig. 3. The function $F_0(z)$ on the right-hand side of (4) is determined by the method of excitation and loading of the probe. When the probe is a *transmitting antenna* driven at its terminals by a voltage $V$, this function becomes

$$F_0(z) = \frac{V}{2} \sin k(h-|z|). \tag{5}$$

When the probe is used as a *receiving antenna* with its terminals short-circuited and the incident field is as shown in Fig. 2(b), $F_0(z)$ becomes

$$F_0(z) = \frac{2jE_0}{k} \sin ks(\cos kz - \cos kh). \tag{6}$$

In (4), $\zeta$ is the wave impedance of the medium

$$\zeta \equiv \omega\mu_0/k \tag{7}$$

and the modified kernel $K_d'$ is

$$K_d'(z,z') = K(z,z') - (\cos kz/\cos kh)K(h,z') \tag{8}$$

where

$$K(z,z') = \frac{e^{-jkR_{11}}}{R_{11}} - \frac{e^{-jkR_{12}}}{R_{12}} \tag{9}$$

and

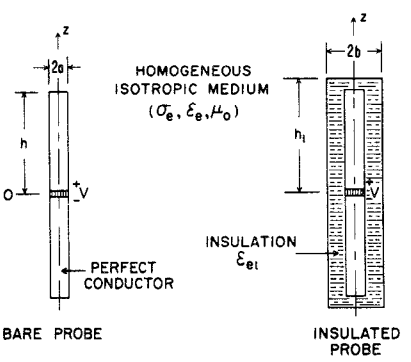


Fig. 3. Details of bare and insulated cylindrical dipole electric-field probes.

$$R_{11} = \sqrt{(z-z')^2 + a^2} \tag{10}$$

$$R_{12} = \sqrt{(z-z')^2 + a^2 + 4s^2}\,. \tag{11}$$

For antennas of length $\beta h \leqq 3\pi/2$ $(h \leqslant 3\lambda/4)$, the following simple expression has been shown to be an accurate representation for the axial current on coupled dipoles in dissipative media [4]:

$$I(z) = e^{-\alpha|z|}\Big[C_1 \sin \beta(h-|z|) + C_2(\cos \beta z - \cos \beta h) + C_3\Big(\cos \tfrac{1}{2}\beta z - \cos \tfrac{1}{2}\beta h\Big)\Big]$$
$$= C_1 f_1(z) + C_2 f_2(z) + C_3 f_3(z). \tag{12}$$

The coefficients $C_1$, $C_2$, and $C_3$ in (12) can be chosen by making the current $I(z)$ satisfy the integral equation (4) as well as possible in the least squares sense [5]. After substituting (12) into (4), the integral equation becomes

$$C_1F_1(z) + C_2F_2(z) + C_3F_3(z) = C_0F_0(z) \tag{13}$$

where

$$F_i(z) = \int_{-h}^{h} f_i(z')K_d'(z,z')\,dz' \qquad (i=1,2,3) \tag{14}$$

and

$$C_0 \equiv j4\pi/\zeta \cos kh. \tag{15}$$

To satisfy the least squares criterion

$$\int_{-h}^{h}\big[C_1F_1(z) + C_2F_2(z) + C_3F_3(z) - C_0F_0(z)\big]^2\,dz = \text{minimum}. \tag{16}$$

The implementation of (16) leads to a set of simultaneous linear equations for the coefficients $C_j (j=1,2,3)$. In matrix form, these equations are

$$[A_{ij}]\{C_j\} = C_0\{B_i\} \tag{17}$$

where

$$A_{ij} = \int_{-h}^{h} F_i(z)F_j(z)\,dz \quad \text{and} \quad B_i = \int_{-h}^{h} F_0(z)F_i(z)\,dz. \tag{18}$$

Once the coefficients $C_j$ are determined by solving the matrix equation (17) with $F_0(z)$ given by both (5) and (6),

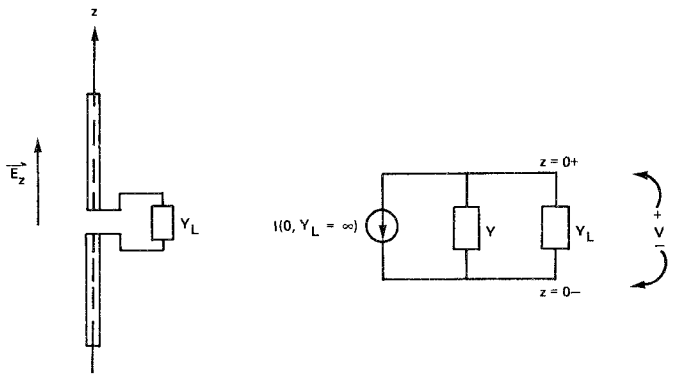


Fig. 4. (a) Loaded receiving probe. (b) Equivalent circuit for loaded probe.

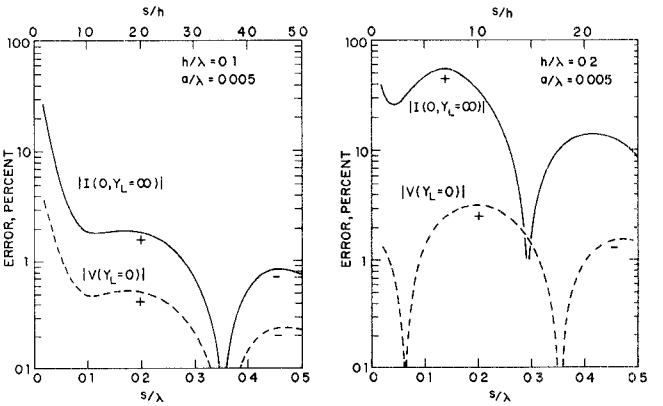


Fig. 5. Errors in short-circuit current and open-circuit voltage for a bare probe in a lossless medium as a function of spacing between probe and interface for two lengths of probe $h/\lambda = 0.1, 0.2$.

it is easy to obtain the input admittance for the driven probe, viz.,

$$Y = \frac{I(0)}{V} \tag{19}$$

and the current at the terminals of the receiving probe when they are short-circuited, viz. $I(0, Y_L = \infty)$. The voltage $V$ across a general load admittance $Y_L$ connected to the terminals of the receiving probe is determined from the equivalent circuit shown in Fig. 4(b)

$$V = -I(0, Y_L = \infty)/(Y + Y_L). \tag{20}$$

When the terminals are open-circuited, this voltage is simply

$$V(Y_L = 0) = -I(0, Y_L = \infty)/Y. \tag{21}$$

The effect the interface has on the response of the probe (the error) can be determined by solving (4) both with and without the presence of the terms representing the image probe (terms which depend on $R_{12}$) and comparing the results. Note that the interaction between the probe and the interface is completely accounted for by the presence of the image probe. With the image probe absent, the voltage at the terminals of the probe as a function of the position $s$ is an exact replica of the standing-wave electric field for $x \leqslant 0$, no matter how close the probe is to the interface. The subscript 0 is used to designate quantities computed with the image probe absent. The errors in the amplitude of the voltage across the load, the amplitude of the open-circuit voltage, and the amplitude of the short-circuit current due to the presence of the interface are then

$$\Delta|V| = \frac{|V| - |V_0|}{|V_0|} = \frac{|I(0, Y_L = \infty)||Y_0 + Y_L|}{|I_0(0, Y_L = \infty)||Y + Y_L|} - 1 \tag{22}$$

$$\Delta|V(Y_L = 0)| = \frac{|I(0, Y_L = \infty)||Y_0|}{|I_0(0, Y_L = \infty)||Y|} - 1 \tag{23}$$

$$\Delta|I(0, Y_L = \infty)| = \frac{|I(0, Y_L = \infty)|}{|I_0(0, Y_L = \infty)|} - 1. \tag{24}$$

## III. Numerical Results

For electrically short receiving probes that are not matched to the load admittance $Y_L$ as is the usual case for the probes used in biological bodies, the errors in the received voltage for two extreme values of the load admittance are of interest, namely, $|Y_L| \ll |Y|$ and $|Y_L| \gg |Y|$. From (22), the error in the received voltage approaches the error in the open-circuit voltage when $|Y_L| \ll |Y|$, i.e.,

$$\Delta|V| \approx \Delta|V(Y_L = 0)| \tag{25}$$

and the error in the received voltage approaches that for the short-circuit current when $|Y_L| \gg |Y|$, i.e.,

$$\Delta|V| \approx \Delta|I(0, Y_L = \infty)|. \tag{26}$$

Numerical results for the errors in these two extreme cases are given in the following examples.

### A. Bare Probe

Fig. 5 shows the errors in both the short-circuit current (24) and the open-circuit voltage (23) for bare probes of two lengths, $h/\lambda = 0.1$, 0.2, as a function of the spacing between the probe and the interface $s/\lambda$. Both probes have the same radius, $a/\lambda = 0.005$, and the medium surrounding the probes is assumed to be lossless, $\alpha/\beta = 0$. The wavelength $\lambda$ is that in the medium surrounding the probe. The errors in the short-circuit current are seen to be substantially greater than those in the open-circuit voltage. The error in the response due to the presence of a nearby interface can, therefore, be decreased by choosing the load admittance such that $|Y_L| \ll |Y|$. A comparison of the results in Fig. 5 for the two lengths of the probe shows that the longer probe generally has a larger error in both the short-circuit current and the open-circuit voltage. An increase in the radius of the bare probe will also increase the error in both the short-circuit current and the open-circuit voltage. This is shown in Fig. 6, where results are presented for probes of length $h/\lambda = 0.1$ and various radii in a lossless medium.

The effect of the dissipation in the medium surrounding the probe on the error in the short-circuit current and the

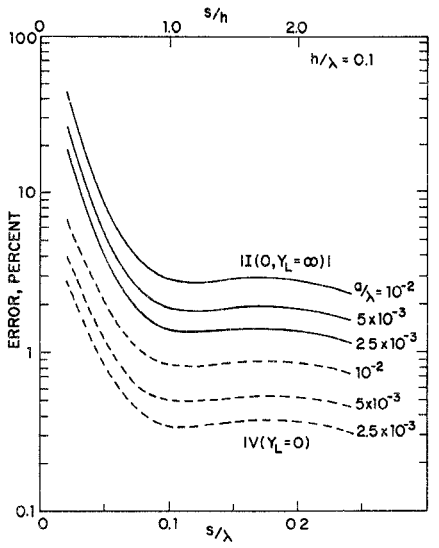


Fig. 6. Errors in short-circuit current and open-circuit voltage for a bare probe in a lossless medium as a function of spacing between probe and interface with radius of probe $a/\lambda$ as a parameter.

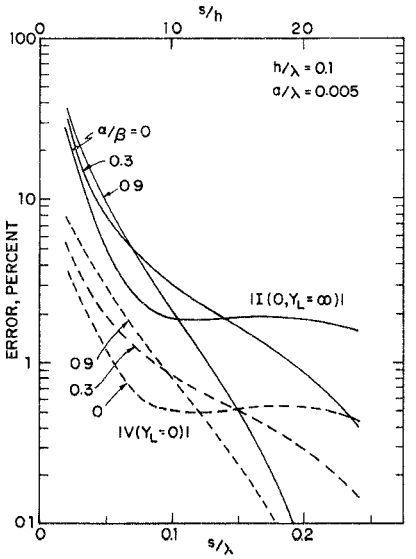


Fig. 7. Errors in short-circuit current and open-circuit voltage for a bare probe in a lossy medium as a function of spacing between probe and interface with ratio $\alpha/\beta$ as a parameter.

open-circuit voltage is examined in Fig. 7 for a bare probe of length $h/\lambda=0.1$. The errors are shown as a function of the spacing between the probe and the interface for three lossy media, $\alpha/\beta=0$, 0.3, 0.9 (effective loss tangent $p_e\approx 0$, 0.66, 9.5). At the larger spacings ($s/\lambda \gtrsim 0.15$), an increase in the ratio $\alpha/\beta$ is seen to decrease the error. This result is consistent with a wave picture for the interaction between the probe and its image; i.e., the attenuation of a plane wave propagating between the probe and the image has its amplitude reduced by a factor of $e^{-2\alpha s}$ due to the dissipation in the intervening medium. When the probe is closer to the interface ($s/\lambda \lesssim 0.05$), an increase in the ratio $\alpha/\beta$ is seen to increase the error. At these close spacings, the wave picture no longer applies. The interaction between

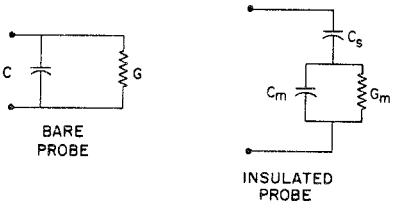


Fig. 8. Circuit representations for the input admittance of electrically short bare and insulated electric-field probes.

the probe and its image is by capacitive and conductive coupling. An increase in the ratio $\alpha/\beta$ causes an increase in the conductive coupling between the probe and the image and, therefore, causes an increase in the error.

### *B. Electrically Short Probe with Concentric Cylindrical Insulation*

When the probe is electrically short and insulated by a concentric dielectric sheath, as in Fig. 3, the approximate analysis presented in [1] can be used to analyze the insulated probe near an interface. As presented in Fig. 8, the previously obtained results show that the input admittance of the electrically short insulated probe $Y_i$ is approximately the admittance of a bare probe, $Y_b = G_m + j\omega C_m$, of length $2h$ and radius $b$, in series with the capacitance of the sheath $C_s$, i.e.,

$$Y_i \approx \frac{j\omega C_s Y_b(b,h)}{Y_b(b,h)+j\omega C_s} \tag{27}$$

where

$$C_s = \pi\epsilon_{ei} h / \ln (b/a) \tag{28}$$

and $\epsilon_{ei}$ is the permittivity of the insulation. The subscripts $b$ and $i$ are used here to identify the quantities associated with the bare and the insulated probes, respectively. For the probe near the interface, the admittance $Y_b$ contains the interaction between the probe and its image and is obtained from the solution of the integral equation (4) with (19). The open-circuit voltage for the electrically short insulated probe $V_i(Y_L=0)$ is approximately the same as that for a bare probe with the same radius $a$ and length $2h$ for the conductor. This voltage can be obtained from the solution of the integral equation (4) with (21):

$$V_i(Y_L=0) \approx V_b(a,h,Y_L=0). \tag{29}$$

The short-circuit current for the insulated probe is then simply

$$I_i(0,Y_L=\infty) = -V_i(Y_L=0)Y_i$$

$$\approx \frac{-V_b(a,h,Y_L=0)j\omega C_s Y_b(b,h)}{Y_b(b,h)+j\omega C_s}. \tag{30}$$

The errors in the short-circuit current and open-circuit voltage for the electrically short insulated probe near an interface can be determined in the same manner as for the bare probe using (24) and (23). The effect of the insulation on these errors is illustrated in Fig. 9 where results are shown for insulated probes with $b/a=3.0$ and $\epsilon_{er}/\epsilon_{eri}=$

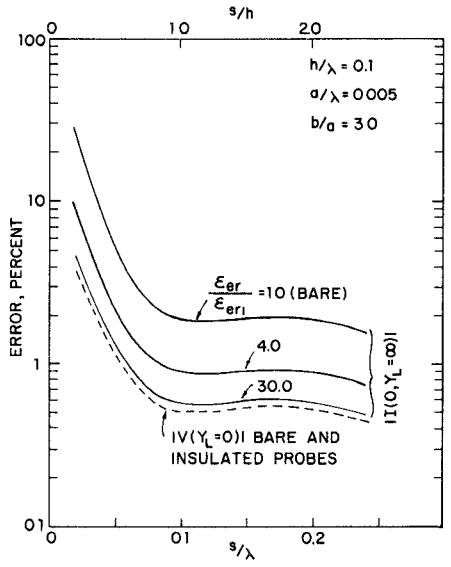


Fig. 9. Errors in short-circuit current and open-circuit voltage for bare and insulated probes in a lossless medium as a function of spacing between probe and interface with ratio $\epsilon_{er}/\epsilon_{eri}$ as a parameter.

1.0 (bare), 4.0 and 30 in a lossless medium. The relative effective permittivities for the medium surrounding the probe and the insulation are $\epsilon_{er}$ and $\epsilon_{eri}$, respectively. The error in the open-circuit voltage is the same for the three different insulations used; this is the result of imposing the equality in (29). The error in the short-circuit current is seen to decrease with an increase in the ratio of the permittivity of the external medium to that of the insulation $\epsilon_{er}/\epsilon_{eri}$ and to approach the error in the open-circuit voltage when this ratio is large. This behavior is easily understood by examining the expression for the admittance of the insulated probe (27). As the ratio $\epsilon_{er}/\epsilon_{eri}$ increases, the admittance of the sheath capacitance $C_s$ decreases relative to the admittance $Y_b$, i.e., $|Y_b(b,h)| \gg \omega C_s$, so that the admittance of the insulated probe is approximately that of the sheath, $Y_i \approx j\omega C_s$. The short-circuit current is then simply proportional to the open-circuit voltage, $I_i(0, Y_L=\infty) \approx -j\omega C_s V_i(Y_L=0)$; therefore, the relative errors in the two quantities $V_i(Y_L=0)$ and $I_i(0, Y_L=\infty)$ are approximately the same. Note that the error in the terminal voltage (22) for all values of the load admittance is also approximately the same as the error in the short-circuit current, $\Delta|V_i| \approx \Delta|I_i(0, Y_L=\infty)|$, when the ratio $\epsilon_{er}/\epsilon_{eri}$ is large, since $Y_{i0} \approx Y_i \approx j\omega C_s$.

## IV. Comparison with Experiment

Before performing experimental measurements for comparison with the theory, an experimental model had to be developed that was a good approximation to the model used in the theoretical analysis. Since the error in the response of the probe due to the nearby interface was a small fraction of the quantity measured, typically $\Delta|V|/|V| = 2$ to 20 percent for the measurements to be described, the experimental model and accompanying instrumentation had to be capable of accurately determining small differences between measured quantities. A geometry that permits an accurate measure of the position of the probe with respect to the interface and a simple characterization of the electric field in the vicinity of the interface were, therefore, essential for the experiment. A section of waveguide filled with a material and terminated in a short circuit was used to model the interface. A small movable monopole probe was inserted through a slot in the center of the upper surface of the waveguide, as shown in Fig. 10. By using the method of images, the response of the monopole probe can be shown to be equivalent to that of the dipole to within a constant factor. With the dominant mode ($TE_{10}$) in the waveguide, the longitudinal distribution of the component of the electric field parallel to the axis of the probe is proportional to sin $(k_g s)$ where $k_g = \beta_g - j\alpha_g$ is the guide wavenumber. This is the same distribution used in the theoretical analysis with the wavenumber in the medium $k$ replaced by $k_g$. If the probe is small compared to the cross-sectional dimensions of the waveguide, i.e., $b < h \ll b_g < a_g$, and is positioned close to the short circuit, i.e., $s \ll a_g/2$, the electromagnetic interaction between the probe and the interface formed by the material medium and the metallic short circuit will be essentially the same as that for the planar geometry with the plane-wave excitation shown in Fig. 2(a). In this case, only the term sin $(ks)$ in (6) must be replaced by sin $(k_g s)$ to obtain theoretical results for comparison with the measured data. Note that the symbols $a_g$ and $b_g$ are used for the cross-sectional dimensions of the rectangular waveguide; the conventional symbols $a$ and $b$ are used to describe the probe.

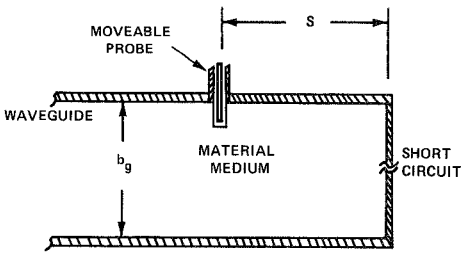


Fig. 10. Detail of experimental arrangement of probe in waveguide.

The error in the voltage measured at the terminals of the monopole probe that is a result of the nearby interface was determined using two different methods. The first method was used when media that were assumed to be lossless were in the waveguide. For a lossless system, the amplitude of the longitudinal standing-wave pattern in the waveguide is repetitive with a period of $\lambda_g/2 = \pi/\beta_g$, where $\lambda_g$ is the wavelength in the guide when it is filled with the medium. The voltages measured at the terminals of the probe when it is positioned at $s$ and $s+\lambda_g/2$ would, therefore, be the same if there were no interaction between the probe and the interface, i.e., the metallic short circuit. When the probe is positioned at $s+\lambda_g/2$, the interface is far enough away that it has a negligible effect on the response of the probe. The error in the response

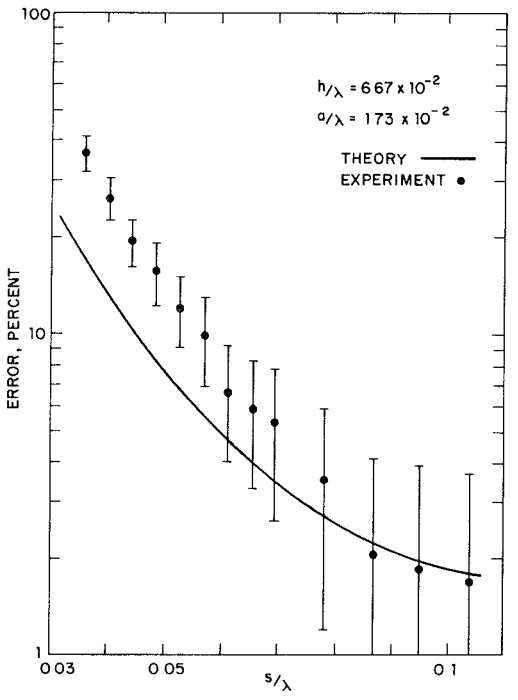


Fig. 11. Comparison of theoretical and experimental results for error in terminal voltage of bare probe in a lossless medium as a function of spacing between probe and interface $|Y_L| \gg |Y|$. $\lambda$ is the wavelength in the medium.

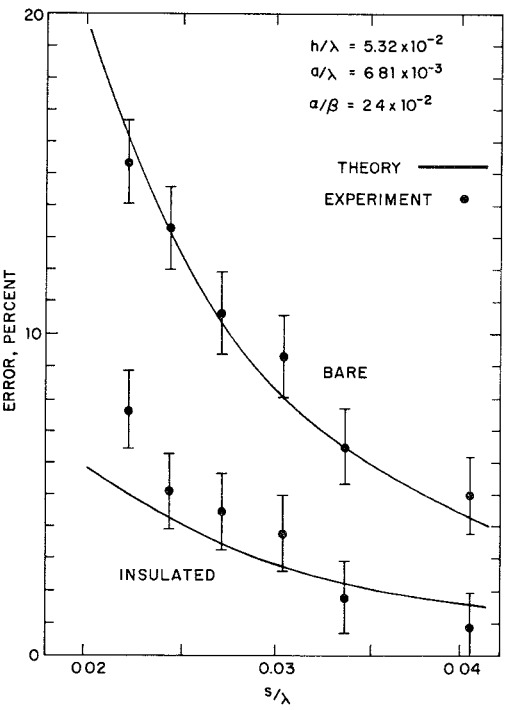


Fig. 12. Comparison of theoretical and experimental results for error in terminal voltage of bare and insulated probes as a function of spacing between probe and interface $b/a \approx 3.28$, $\epsilon_{er}/\epsilon_{eri} \approx 37$, $|Y_L| \gg |Y|$. $\lambda$ is the wavelength in the medium.

$\Delta|V(s)|$ can, therefore, be determined from the voltages measured with the probe positioned at $s$ and $s+\lambda_g/2$, i.e.,

$$\Delta|V(s)| = \frac{|V(s)| - |V(s+\lambda_g/2)|}{|V(s+\lambda_g/2)|} = \frac{|V(s)|}{|V(s+\lambda_g/2)|} - 1. \tag{31}$$

A second method for measuring the error $\Delta|V(s)|$ was used with lossy media in the waveguide. The voltage at the terminals of the probe is measured as a function of the position $s$. At a point $s'$ away from the interface (typically $s' = \lambda_g/4$), the interaction between the probe and the interface is assumed to be negligible, so that $\Delta|V(s')| = 0$. The error in the response at distances closer than $s'$ to the interface is then determined from

$$\Delta|V(s)| = \frac{|V(s)||\sin k_g s'|}{|V(s')||\sin k_g s|} - 1. \tag{32}$$

In Fig. 11, theoretical and experimental results for the error $\Delta|V(s)|$ are displayed as a function of the position $s/\lambda$ for a bare probe with the dimensions $h/\lambda = 6.67 \times 10^{-2}$, $a/\lambda = 1.73 \times 10^{-2}$. $\lambda$ is the wavelength in the infinite medium and not to be confused with the guide wavelength $\lambda_g$. The medium in the waveguide for the experiment was air, which was assumed to be lossless, and the frequency of operation was 10 GHz. The load admittance at the terminals of the probe was chosen so that $|Y_L| \gg |Y|$. The error brackets for the measured data were determined by considering both the errors associated with the positioning of the probe and the metering of the voltage. The rather large errors associated with the quantity $\Delta|V(s)|$ are the result of the manner in which errors in the measurement of $|V(s)|$ enter the calculation of $\Delta|V(s)|$. The numerator of (31) is the difference between two measured quantities that are nearly equal; a small error in either number will, therefore, give a large error in the result. For example, if $\Delta|V(s)|$ is approximately 0.1, a $\pm 1$-percent error in the measurement of $|V(s)|$ can cause an error as large as $\pm 20$ percent in $\Delta|V(s)|$. The overall agreement between the theoretical and experimental results in Fig. 11 is seen to be good. The differences that do exist between the theoretical and the experimental results at the closer spacings (smaller values of $s/\lambda$) are possibly due to the proximity effect which makes the distribution of the surface current around the circumference of the probe nonuniform [6]. This effect, which is not considered in the present analysis, causes the effective separation between the probe and its image to be slightly less than the actual separation, and thus causes an increase in the error $\Delta|V(s)|$ over that which is computed without considering the proximity effect.

In Fig. 12, theoretical and experimental results for the error $\Delta|V(s)|$ are displayed as a function of the position $s/\lambda$ for a bare probe and the same probe with an insulating sheath. The dimensions of the probes are $h/\lambda = 5.32 \times 10^{-2}$, $a/\lambda = 6.81 \times 10^{-3}$, and the insulation is formed from Teflon, $\epsilon_{er} \approx 2.1$, $b/a = 3.28$. The medium in the waveguide for this experiment was fresh water. At the frequency of operation, 900 MHz, the relative effective permittivity and effective loss tangent of the water are $\epsilon_{er} \approx 78$, $p_e \approx 4.8 \times 10^{-2} (\epsilon_{er}/\epsilon_{eri} \approx 37$, $\alpha/\beta \approx 2.4 \times 10^{-2})$. Note that the section of WR90 waveguide used here was

the same as in the previous experiment. The frequency of operation was lowered to compensate for the increase in the electrical size of the guide that resulted from replacing the air by fresh water. The load admittance at the terminals of both probes satisfies the inequality $|Y_L| \gg |Y|$. The overall agreement between the theoretical and experimental results is seen to be good. The reduction in the error due to adding the insulation is clearly displayed.

## V. Other Forms of Insulation

The theoretical and experimental results presented here and in the previous paper [1] are for the linear antenna with a concentric cylindrical insulation. In certain applications it may be desirable to use an insulation with another shape. For example, for isotropic probes constructed from three orthogonal dipoles, such as those used in biological tissue, the insulation may be a dielectric sphere that encapsulates all three probes [7], [8]. A complete analysis is not available for the linear antenna with an insulation of general shape. The following approximate analysis suggests, however, that the behavior of all insulated dipole probes with dimensions that are small compared to the wavelength in the surrounding medium will be similar to that for the probe with a concentric cylindrical insulation.

The voltage developed across the load admittance $Y_L$ at the terminals of the dipole when it is in an incident field $E_z$ parallel to its axis is

$$V = K_e E_z = V(Y_L = 0) \frac{Y}{Y + Y_L} \tag{33}$$

where $V(Y_L = 0)$ is the voltage at the terminals when they are open-circuited. For an arbitrary load admittance $Y_L$, the voltage response (33) will be independent of the electrical properties of the external medium $(\sigma_e, \epsilon_e, \mu_0)$ only if the input admittance $Y$ of the driven probe and the term $V(Y_L = 0)$ are both independent of these properties.

The input admittance of an insulated dipole that is electrically short in the external medium can be represented by the equivalent circuit shown in Fig. 8. The relative magnitudes of the elements in this circuit will depend upon the shape of the insulation and the electrical properties of the insulation and the external medium. When the insulation is not very thin (referring to Fig. 13, the radius of the insulation should be much greater than the radius of the wire, $b \gg a$) and the relative permittivities satisfy the inequality $\epsilon_{er}/\epsilon_{eri} \gg 1$, the admittance due to the insulating sheath will be much less than that for the elements that represent the external medium (parallel combination of $G_m$ and $C_m$). In this event, the input admittance of the dipole will be approximately that of the sheath capacitance $Y \approx j\omega C_s$, and will be independent of the properties of the external medium. This is the same as the behavior exhibited by the input admittance of the electrically short dipole with a concentric cylindrical insulation when $\epsilon_{er}/\epsilon_{eri} \gg 1$.

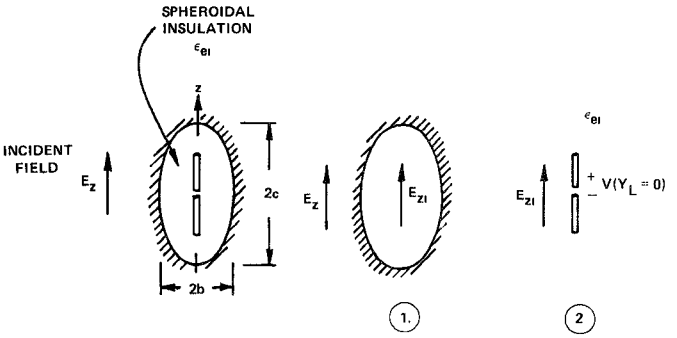


Fig. 13. Dipole with prolate spheroidal insulation showing steps in the approximate analysis.

In general, the open-circuit voltage $V(Y_L = 0)$ for the insulated dipole will be a complicated function of the shape of the insulation and the electrical properties of the insulation and the external medium. The following *approximate* analysis, however, can be used to show that the voltage $V(Y_L = 0)$ for the electrically short probe will be nearly independent of the electrical properties of the external medium for a large range of insulator shapes when the ratio of permittivities satisfies the inequality $\epsilon_{er}/\epsilon_{eri} \gg 1$.

Consider the linear dipole with an insulation formed by a solid dielectric in the shape of a coaxial prolate spheroid; see Fig. 13. When the dimensions of the dipole are small compared to those of the insulation, the analysis of this structure can be approximately divided into two parts. First, the electric field $E_{zi}$ at the center of the prolate spheroid is determined with the dipole absent. The open-circuit voltage at the terminals of the dipole is then determined from the simple relation for an isolated electrically short dipole in an infinite medium with the electrical properties of the insulation and the incident field $E_{zi}$, viz., $V(Y_L = 0) = -hE_{zi}$. This simple analysis, of course, neglects the interaction (multiple scattering) between the dipole and the dielectric discontinuity at the surface of the insulation.

When the spheroid is electrically small in the external dielectric medium, the internal axial field $E_{zi}$ is approximately that obtained from an electrostatic analysis [9], and the resulting open-circuit voltage is

$$V(Y_L = 0) \approx -hE_{zi} = -hE_z \left\{ 1 + \left( \frac{\epsilon_{eri}}{\epsilon_{er}} - 1 \right) (\chi^2 - 1) [\chi \operatorname{ctnh}^{-1}(\chi) - 1] \right\}^{-1} \tag{34}$$

where

$$\chi = c/\sqrt{c^2 - b^2} \tag{35}$$

and $b$ and $c$ are the semiaxes of the spheroid. For a long thin spheriodal insulation $c \gg b$, (34) reduces to

$$V(Y_L = 0) = -hE_z \tag{36}$$

which is the same as the open-circuit voltage obtained for the electrically short dipole with a concentric insulation,

cf., [1, (17)] with $Y_l=0$. The other limiting case for the prolate spheroid occurs when $b=c$, i.e., the insulation is a dielectric sphere. For a spherical insulation (34) reduces to

$$V(Y_L=0)=-hE_{z_l}=-hE_z\frac{3\epsilon_{er}}{2\epsilon_{er}+\epsilon_{eri}}. \qquad (37)$$

Note that for any value of the ratio of the axes of the spheroid ($0 \leqslant b/c \leqslant 1$), a large value for the ratio of the permittivities $\epsilon_{er}/\epsilon_{eri} \gg 1$ will make the open-circuit voltage (34) independent of the permittivity of the external medium $\epsilon_{er}$.

In summary, the approximate analysis presented above suggests that the voltage response (33) of an electrically small dipole with a general shape for the insulation will be independent of the electrical properties of the external medium whenever the insulation is not very thin and the inequality $\epsilon_{er}/\epsilon_{eri} \gg 1$ is satisfied. This is the same behavior that was shown both theoretically and experimentally to be true for the electrically short dipole with a concentric cylindrical insulation.

## VI. Summary and Discussion

A "worse case" analysis has been formulated to determine the effect of a nearby interface on the response of an electric field probe. In summary, the results of this simple analysis show that the interaction between the electrically short probe and the interface has the following properties:

a) The interaction (error in the response) is decreased if the radius or the length of the probe is reduced.

b) A low value for the load admittance at the terminals of the probe, i.e., $|Y_L| \ll Y$, will produce less interaction (error in the response) than a high value of the load admittance, i.e., $|Y_L| \gg |Y|$.

c) An increase in the dissipation ($\alpha/\beta$) in the medium surrounding the probe will decrease the interaction (error in the response) at a distance from the interface, but can increase the interaction when the probe is very close to the interface.

d) The use of a probe with a concentric cylindrical insulation of permittivity ratio $\epsilon_{er}/\epsilon_{eri} \gg 1$ can reduce the interaction (error in the response) to the level that is obtained with an open-circuited bare probe with the same dimensions, and the interaction, for the insulated probe, unlike that for the bare probe, will be independent of the value of the load admittance used.

e) For electrically short bare probes that are thin ($h/\lambda \leqslant 0.1$, $a/h \leqslant 0.1$), the error in the response for either load condition ($|Y_L| \ll |Y|$, $|Y_L| \gg |Y|$), was found to be less than 5 percent when the distance from the interface was greater than the half-length of the probe $s \gtrsim h$. For the cases examined, the addition of an insulating sheath with $\epsilon_{er}/\epsilon_{eri} \gg 1$ reduced the error to less than 5 percent for spacings $s \gtrsim h/3$.

A simple approximate analysis indicates that the response of all electrically short insulated dipole probes will exhibit a behavior similar to that for the probe with a concentric cylindrical insulation when the insulation is not very thin and the permittivity ratio $\epsilon_{er}/\epsilon_{eri} \gg 1$. A more comprehensive analysis of the dipole with an insulation of general shape is clearly needed.

In a recent report, Cheung has presented measured data for the electric field near an interface that were taken using an electric-field probe developed by the United States Bureau of Radiological Health (BRH) [10]. The planar interface in this experiment was formed by air and a slab of simulated muscular tissue with the electrical properties $\epsilon_{er} \approx 50$, $p_e \approx 0.35$ at the frequency of operation 2.45 GHz. The dipole elements of the BRH probe are insulated and have a half-length of about $h=1.25$ mm. At the operating frequency, $h/\lambda \approx 7.3 \times 10^{-2}$ in the simulated muscular tissue. No error was detected in the response of the probe as it was moved through the muscular material toward the interface (decreasing $s$). The scatter in the measured data, however, is about $\pm 10$ percent for a group of measurements made at a fixed distance from the interface, cf., [10, fig. 13]. The findings are in agreement with the present analysis, since the analysis predicts an error in the response of less than 4 percent at spacings $s \geqslant h$ for a *bare* probe with the same dimensions as the BRH probe and the terminals short-circuited, i.e., $|Y_L| \gg |Y|$. The error in the response due to the presence of the interface was, therefore, undetectable since it was probably less than the scatter in the measured data. In fact, the error in the response for the BRH probe was probably less than 4 percent when $s \geqslant h$, because the insulation on the probe and the large value used for the load admittance reduced the error below that for the bare probe with $|Y_L| \gg |Y|$, as is shown by the present analysis.

## References


[1] G. S. Smith, "A comparison of electrically short bare and insulated probes for measuring the local radio frequency electric field in biological systems," *IEEE Trans. Biomed. Eng.*, vol. BME-22, pp. 477–483, Nov. 1975.

[2] G. S. Smith and R. W. P. King, "Electric field probes in material media and their use in EMC, "*IEEE Trans. Electromagn. Compat.*, vol. EMC-17, pp. 206–211, Nov. 1975.

[3] H. I. Bassen and A. Cheung, "Comment on experimental and theoretical studies on electromagnetic fields induced inside finite biological bodies" (with reply by K. M. Chen), *IEEE Trans. Microwave Theory Tech.*, vol. MTT-25, pp. 623–624, July 1977.

[4] S. R. Mishra, L. D. Scott, and R. W. P. King, "Currents, charges, and admittances of linear antennas in dissipative media," *Radio Sci.*, vol. 9, pp. 487–495, Apr. 1974.

[5] F. B. Hilderbrand, *Methods of Applied Mathematics*. Englewood Cliffs, NJ: Prentice-Hall, 1952, pp. 452–459.

[6] G. S. Smith, "Proximity effect in systems of parallel conductors," *J. Appl. Phys.*, vol. 43, pp. 2196–2203, May 1972.

[7] H. Bassen, W. Herman, and R. Hoss, "EM probe with fiber optic telemetry," *Microwave J.*, vol. 20, pp. 35–39, Apr. 1977.

[8] H. Bassen, P. Herchenroeder, A. Cheung, and S. Neuder, "Evaluation of an implantable electric-field probe within finite simulated tissues," *Radio Sci.*, vol. 12, pp. 15–25, Nov.–Dec. 1977.

[9] E. Weber, *Electromagnetic Theory*. New York: Dover, 1960, pp. 504–509.

[10] A. Y. Cheung, "Electric field measurements within biological media," in *Proc. Conf. on Biological Effects and Measurements of Radio Frequency/Microwaves* (Rockville, MD), pp. 117–135, HEW Publication (FDA) 77-8026, July 1977.